Photon Netw Commun (2012) 24:237–251
DOI 10.1007/s11107-012-0384-9

Novel strategies for sparse regenerator placement in translucent optical networks

Daniel A. R. Chaves · Renan V. B. Carvalho · Helder A. Pereira · Carmelo J. A. Bastos-Filho · Joaquim F. Martins-Filho

Received: 27 January 2012 / Accepted: 19 April 2012 / Published online: 11 May 2012

Abstract In this paper, we propose two strategies for sparse regenerator placement (*RP*) in translucent optical networks, named most used regenerator placement (MU-RP), and most simultaneous used regenerator placement (MSU-RP). Our proposals are compared to well known *RP* algorithms presented in literature for two different network topologies for different network loads, distribution of load along the networks and number of translucent nodes. MSU-RP presented remarkable results and outperformed all previous approaches in all cases, while MU-RP obtained a slightly superior or similar performance when compared to previous approaches presented in the literature.

Keywords Optical networks · Translucent optical networks · Sparse regeneration · Regenerator placement · Regenerator allocation

D. A. R. Chaves · H. A. Pereira · C. J. A. Bastos-Filho
Polytechnic School of Pernambuco, University of Pernambuco, Recife, PE, Brazil
e-mail: daniel.rchaves@ufpe.br

H. A. Pereira
e-mail: helder.pereira@poli.br

C. J. A. Bastos-Filho
e-mail: carmelofilho@ieee.org

R. V. B. Carvalho · J. F. Martins-Filho (✉)
Department of Electronics and Systems,
Federal University of Pernambuco, Recife, PE, Brazil
e-mail: jfmf@ufpe.br

1 Introduction

Optical networks emerged as a promising solution to provide infrastructure to deal with the ever-growing bandwidth demand generated by the recent released telecommunications services [1].

In the first generation of optical networks, all the network nodes were opaque. This means that an optical to electrical and an electrical to optical conversion (O/E/O) has to be accomplished in all nodes of the lightpath, i.e. the optical signal needs to be converted to the electrical domain at each node of the lightpath, then the signal has to be electronically processed and reconverted to the optical domain [2]. These networks require an excessive number of O/E/O interfaces, which increases the overall capital expenditure (CAPEX) and operational expenditure (OPEX) of the network. The CAPEX is related to the cost of these interfaces, while the OPEX is related to the energy consumption and the maintenance issues. On the other hand, these O/E/O interfaces permit to restore the quality of the optical signal by performing re-amplification, re-formating and re-timing (3R regeneration) [2].

An alternative to the opaque networks is to avoid the use of O/E/O interfaces by routing the signal in the optical domain along the core nodes. This solution is referred in the literature as all-optical networks or transparent optical networks [2]. In these networks, the optical signal propagates from the source node to the destination node with no O/E/O conversion. In general, all-optical networks present lower CAPEX and OPEX, but are more susceptible to the impairments imposed by the physical layer. It occurs since no 3R regeneration is performed and the penalties generated by the impairments are accumulated for several fiber spans and devices.

Translucent optical networks (TON) can be viewed as an interesting solution to deal with this trade-off, by balancing

network performance and CAPEX/OPEX [3]. TONs are planned to just have some of the nodes with regeneration capabilities and can be classified in two categories according to the strategy to deploy the regenerators in the network [3]: islands of transparency and sparse regeneration.

The first one aims to create islands of transparency [3–5], in which all the nodes that belong to a given island are transparent and do not present any regeneration capability. Cross-connectors with regeneration capability are located only in the nodes positioned on boundaries of the island. The main problem of this approach is to properly define the clusters of transparent nodes [4].

The sparse regeneration refers to the strategical distribution of the regeneration capability by selecting a set of nodes along the network to place these devices [3,6]. These regenerators are used to perform 3R signal regeneration when it is necessary [6,7]. In this paper, we are concerned with the sparse placement approach since we believe it can yield to more appropriate and cost-effective use of the regeneration resources.

To use the sparse approach, one needs to use a regenerator placement (*RP*) algorithm [3]. The RP algorithm decides which nodes should be translucent and the number of regenerators that should be installed in each of these nodes. The *RP* problem takes place during the network design and is classified as a NP-complete problem [3]. In the theory of computational complexity, the NP-complete class consists of the decision problems for which no deterministic algorithm with a polynomial complexity is known to solve the problem. This means that the time (or number of steps) required to find the optimal solution to such problems grows exponentially as the number of input variables of the problem increases. If no property of the function under optimization is know in advance, the optimal solution for these problems might require an exhaustive search (i.e. testing all possible inputs). An exhaustive examination of all RP solutions requires:

$$\prod_{i=1}^{N}((G(i)\cdot W)+1) \tag{1}$$

evaluations, where N is the number of the network nodes, $G(i)$ is the node degree of the ith network node and W is the number of wavelengths in the network. This number of evaluations clearly grows exponentially with the number of nodes N.

One might try to find the optimal solution for the RP problem by using some tool provided by the operational research (mathematical programming). In this paper, we consider the case of the optimization of the network blocking probability as a function of the number of regenerators placed in the network, assuming a dynamic traffic. Since, in general, the network blocking probability is a non-linear function of the number of regenerators placed in the network, no integer linear programming (ILP) technique can be applied in this scenario. Instead, a non-linear integer programming technique, which requires a prohibitive computational time if no property of the function under optimization is know in advance, should be applied to deal with this problem. Since no a priori information is known about the blocking probability function, finding the optimal solution to the RP problem could be computationally infeasible even considering a small number of input variables.

In order to tackle the RP problem in the considered scenario, two approaches can be used: an approximation algorithm or a heuristic algorithm. The first provides an algorithm that ensures a nearly optimal solution for some NP-complete problem with a reduced computational complexity compared to the original problem. The second makes use of information or insight about the problem to solve it quickly. Both strategies allow solving computationally complex problems in a reasonable time frame. However, these strategies do not guarantee that the obtained solution is an optimal solution.

Recently, Flammini et al. [8] investigated the computational complexity of the RP problem for a network with a static traffic. The authors declare that there is no approximation algorithms for solving the RP problem that assumes a restriction on the number of the regenerators available to be placed in the network. This is exactly the case we are dealing with in the present paper. Moreover, we are studying the RP problem considering a dynamic traffic environment, which is much more challenging than the static traffic considered in [8]. Because of these issues, we are using heuristic approaches to solve the RP problem in this paper.

Most of the *RP* algorithms presented in the literature are focused solely on the network topology or on the network traffic distribution [6]. The topology-based *RP* algorithms consider only the network topology information, such as: the number of nodes and links, the node degree, the static physical impairments information, among others [6,9]. These approaches can be easily implemented, but in general do not return solutions that present high network performance. It occurs since the network can be submitted to a wide variety of traffic patterns, which were not considered during the placement process. On the other hand, the *RP* algorithms based on the traffic load distribution determine the locations of the regenerators based on the traffic load information [6]. These strategies are usually more time consuming, but yield better network performances for the load distribution used during the optimization process.

The physical layer information should be used to decide the regenerator locations in order to obtain an optimum solution. This can be done by evaluating directly the optical physical impairments [10] or by determining the maximum optical transparent reach (MOTR), which is the maximum distance that an optical signal can reach without needing regeneration [11]. In a scenario where the traffic load varies, the

MOTR is only an approximation, since the MOTR of a given lightpath may change, dynamically, over the time.

In a scenario in which the connection are dynamically requested to the network (considered in this paper), the control plane must decide on-the-fly when and in which node a signal must be regenerated. This problem is known as regeneration assignment [9] or regeneration allocation [6] (*RA*). One should observe that there might be multiple nodes with regeneration capability along the lightpath. The *RA* algorithm must decide at which nodes of the route the optical signal must regenerated. An efficient *RA* uses as few regenerators as possible, leaving these assets free to attend future regeneration needs. One should observe that an efficient *RA* algorithm may even reduce the minimum number of regenerators needed to maintain the performance, thus leading to a lower CAPEX.

The *RA* algorithm may split a given route in a chain of several transparent segments. Each of these transparent segments may not have the same wavelength, which characterizes a wavelength conversion [6]. This feature can be used to deal with lack of resources. For example, when the same wavelength is not available in all links that belongs to a lightpath. We name this case regeneration triggered by the wavelength contention (tWC). The *RA* algorithm can also be triggered, that is, find an available regenerator in the route, when the quality of the signal is below a predefined threshold. We name this case regeneration triggered by unacceptable signal quality of transmission ($tQoT$).

In this paper, we propose three heuristic algorithms for translucent networks using 3R regeneration: one for the *RA* problem and other two to deal with the *RP* problem. In the Sect. 2, we review some previous *RP* algorithms. In Sections 3 and 4, we present our proposals to tackle the *RA* and the *RP* problems, respectively. Section 5 describes the simulation setup. The simulations results are presented and discussed in Sect. 6. Finally, we give our conclusions in Sect. 7.

2 Previous works

In this section, we review some strategies for regenerator placement reported in the literature. Most of the heuristic RP algorithms for dynamic traffic reported in the literature are based on two main ideas: node counter and ranking (*NC&R*) and transitional weight (TW) [12]. These strategies are usually used jointly.

In the *NC&R* strategy, a dedicated counter is assigned for each network node. The counter is incremented depending on the heuristics used by the RP algorithm. At the end of the process, the nodes that the counter presents higher values are selected for placement (ranking). The most used node selection and placement strategy is the *NX-policy* [6,9,12,13]. The *NX-policy* stands for the class of RP algorithms that assume as the algorithm input information about the number of desired translucent nodes (N) and the number of regenerators to be placed in each selected node (X). The TW is often used as counter increment strategy. The TW assumes a given routing algorithm and each time a route passes thought a given node the counter of this node is incremented or not according to the heuristics used. There is the *Topology-TW* strategy, where only one route linking all possible pairs of source and destination nodes are considered, and there is the *Traffic-TW* strategy, where a given traffic matrix is considered during the algorithm evaluation.

Yang and Ramamurthy [14] proposed four heuristic algorithms to solve the RP problem. Two algorithms are based on the network topology: static with random (SWR) and static with topology (SWT), whereas the other two are based on the traffic: dynamic with load (DWL) e dynamic with BER (DWB). The SWT, DWL and DWB are *NC&R* algorithms. The SWT tries to identify the most centralized node. DWL and DWB use the *Traffic-TW* strategy for node counter incrementation and the node counters are incremented by a number that is, respectively, the order of the giving node in the route and the bit error rate measured in the given node in the route.

Ye et al. [12] proposed three heuristic RP strategies based on the network topology. The first strategy is purely the *Traffic-TW* with *NC&R* with the node counter incremented every time a route traverses a given node. The second strategy ranks the nodes according to the longest link attached to the given node. The third is a combination of the two previous approaches.

Yang and Ramamurthy [6] proposed four heuristic RP algorithms, two based on the network topology: nodal degree first (NDF) and centered node first (CNF), and two based on the network traffic: signal quality prediction based (SQP) and traffic load prediction based (TLP). The NDF algorithm places regenerators in the nodes with higher node degree. CNF is similar to the SWT with a different metrics. The SQP algorithm applies both *NC&R* and *Traffic-TW*. The counters of the jth node and its neighbors in a given route are incremented each time a multiple of the maximum transparent reach in terms of hops is exceeded. The TLP algorithm is similar to the first algorithm in [12] with small differences. Yang and Ramamurthy recommended to use of NDF and SQP since they achieved the best performance among the algorithms investigated in [6]. We use SQP and NDF algorithms for the sake of comparison to our proposals in the present paper.

Peng et al. [13] proposed a RP algorithm named regeneration weight (RW). The RW is similar to SQP; however, it considers the transparent reach in terms of both maximum physical length and maximum number of hops.

Sambo et al. [15] proposed the multiple path signal quality prediction (MPSQP), which was derived from SQP. The

MPSQP is based only in the topology and it considers a set of candidate routes linking each source-destination pairs. It is a *Topology-TW* with *NC&R* algorithm.

All these previous algorithms were used or can be used along with the *NX-policy*.

Chaves et al. [16,17] proposed a meta-heuristic RP algorithm based on a multi-objective evolutionary algorithm, which considers both network cost and number of regenerators as optimization targets.

In this paper, we investigate the regenerator placement in optical networks subjected to dynamic traffic. Due to the stochastic nature of the dynamic traffic, the optimum solution for the regenerator placement when an optimization target is set might only be possible in terms of probabilities. On the other hand, there has been some recent reports on solutions for the regenerator placement problem for either incremental traffic [18–20] or static traffic [8,21–24]. For these two cases, the traffic matrixes are know in advanced and for this reason the optimum solution of the problem can be formulated and achieved (although in many cases it requires a prohibitive processing time).

In this paper, we propose two heuristic RP algorithms based on network traffic, named MU-RP and MSU-RP. Both algorithms use the *NC&R* and *Traffic-TW* strategies. MU-RP uses the *NX-policy*, whereas MSU-RP does not. All the surveyed RP algorithms try to infer where are the best nodes to place the regenerators, not using the information of where the signal regeneration is actually necessary. MU-RP and MSU-RP assume an unlimited number of regenerators in each network node, while they are deciding which nodes should be provided with regeneration capabilities. By doing this, we believe the node counter can retrieve the information about the regeneration usage in a high-performance scenario. Thus, the RP algorithms can place the regenerators in network nodes as close as possible for this best scenario, considering a given limited number of regenerators to be placed in the network.

3 Sparse regenerator placement proposals

We propose two traffic-based regenerator placement algorithms. In both algorithms, the decision about the number of regenerators that should be installed in each node is based on an offline simulation. The offline simulation consists in the execution of a large set of dynamic call requests in a fully opaque network (i.e., each node of the network is provided with an unlimited regeneration capabilities). The strategy is to allow the network to work in the ideal case and to retrieve information about the best nodes to place the regeneration. It allows one to discover the bottleneck nodes, in terms of regeneration, when the constraints are not being considered. One should observe that this unlimited capacity is considered solely during the RP process. The performance analysis carried out in the Sect. 6 is performed using the number of regenerators determined by the RP Algorithms. Furthermore, we assume a shared pool of regenerators [6] in the translucent node architecture in this paper.

The first algorithm is named most used regenerator placement (MU-RP) and the pseudocode is provided in Algorithm 1. It uses the *NX-policy*, which means it places the same number X of regenerators in the N most requested nodes for regeneration during the offline simulation. The X and N are input parameters for MU-RP. This algorithm sets a counter for each network node. This counter is initiated with zero for all nodes. A large number of call requests (i.e. 100,000 call requests) are simulated considering a given traffic load distribution along the network. Each time the RA algorithm decides to use a regeneration in a given node i, the counter of this node is incremented. After the last call request, the N nodes with higher counting values receive X shared regenerators.

Algorithm 1 MU-RP(N,X)

1: Set $R_i \leftarrow 0$ for each node in the network.
2: Start an offline simulation (dynamic traffic) considering all network nodes with an unlimited number of regenerators.
3: **for** Each call request **do**
4: Run the Translucent CAC algorithm (Algorithm 3).
5: **if** (The RA decides regenerate the signal at the node i) **then**
6: $R_i \leftarrow R_i + 1$.
7: **end if**
8: **end for**
9: Place X regenerators in the N nodes that have the higher values of R_i.

The second algorithm is named as maximum simultaneously used regenerator placement (MSU-RP). It distributes R regenerators over the network based on the maximum instantaneous number of regenerators used in each node during the offline simulation. The total number of regenerators to be placed in the network R is an input for MSU-RP instead of X and N as in MU-RP. Note that we can perform a fair comparison between MU-RP and MSU-RP algorithms by setting $R = N \cdot X$, since $N \cdot X$ is the total number of regenerators placed in the network by MU-RP. The MSU-RP algorithm sets a counter for each network node. This counter R_i is initialized with zero for all nodes. A large number of call requests (i.e. 100,000 call requests) are simulated considering the unlimited regeneration capabilities and a given traffic load distribution. Each time the RA algorithm decides to use a regenerator in a given node i, the counter R_i of this node is assigned with a number according to the current number of regenerators $r(i)$ used in node i. The $r(i)$ function returns the current number of regenerators assigned to lightpaths at the node i. For a better understanding of the meaning of the

$r(i)$ function, suppose that there are 10 regenerators installed at the node i. If in a given instant of time, the node i has 6 idle regenerators and 4 regenerators being used by lightpaths passing through this node, then $r(i)$ returns 4. Thus, the value returned by the $r(i)$ function depends on the current network state and may vary along the time since we are dealing with a dynamic traffic. If current number of used regenerators at node $i(r(i))$ is greater than the counter R_i, the counter R_i is assigned with $r(i)$ otherwise, the counter R_i remains unaltered. Using this strategy, it is possible to know the maximum number of regenerators simultaneously used in a given node. This number is stored in the R_i counter at the end of the offline simulation. For example, if at the end of the offline simulation R_i equals 6, it is not worth placing 10 regenerators at the node i, since it used, at most, 6 regenerators simultaneously during the offline simulations. Thus, to place the regenerators taking into account this worst case should be good strategy. After the last call request, each node has stored in its R_i counter the worst case of regenerators use. Then, R regenerators given as input for MSU-RP are proportionally distributed among the network nodes according to the R_i of each node. The MSU-RP can be implemented using the pseudocode shown in Algorithm 2. In this pseudocode, the $r(i)$ is the current number of regenerators used at node i, n is the total number of nodes in the network, and the function $ROUND(w)$ returns the nearest integer to w.

Algorithm 2 MSU-RP(R)

1: Set $R_i \leftarrow 0$ for each node in the network.
2: Start an offline simulation (dynamic traffic) considering all network nodes with an unlimited number of regenerators.
3: **for** Each call request **do**
4: Run the Translucent CAC algorithm (Algorithm 3).
5: **if** (The RA decides regenerate the signal at the node i) **then**
6: $R_i \leftarrow max(R_i, r(i))$ {$r(i)$ returns the current number of regenerators assigned to lightpaths at node i }
7: **end if**
8: **end for**
9: Place $ROUND(R \cdot R_i / \sum_{i=1}^{n} R_i)$ regenerators at node i.

4 Regenerator allocation

The regenerator allocation (RA) algorithm is responsible for determining at which nodes the optical signal must be regenerated in a given lightpath. In this section, we propose a RA algorithm that consists of small modifications in the algorithms proposed in [6,12,25]. Our RA algorithm differs from these algorithms because it assigns a wavelength before the route segmentation and the RA process is triggered by either wavelength contention or unacceptable signal quality.

In our approach, we assume that the RA is invoked after the RWA procedure. Moreover, since the focus of this paper is the study of the RP algorithms, we selected simple algorithms to solve the RWA problem: the Dikstra's shortest path algorithm for routing and the first-fit algorithm for wavelength assignment (WA). However, virtually any other more sophisticated RWA could be used along with our proposal.

Our RA algorithm is able to deal with three possible cases for a given route: the lightpath can be established in all-optical manner (no regeneration is needed), a wavelength conversion is needed to established the lightpath (the regeneration is triggered by the wavelength contention) or an electronic regeneration is needed in order to establish the incoming call request due to unacceptable signal QoT (regeneration triggered by unacceptable signal quality). The translucent call admission control (translucent CAC) identifies which case have occurred and triggers the proper RA strategy to deal with this incoming case. The pseudocode for the translucent CAC is shown in Algorithm 3. The first step of the translucent CAC after the arrival of a call request is the execution of the the routing algorithm which returns a route π ($\pi = \{t_1, t_2, \ldots, t_Z\}$), composed by Z nodes linking the source node (t_1) to the destination node (t_Z). Note that the t_i is the node index in the network, whereas i stands for the position of the node t_i in the π route. Then, the WA algorithm (first fit) is applied to the selected route π in order to assign an available wavelength. The WA algorithm can succeed or not depending on the wavelength availability in the network. If the WA algorithm succeeds in finding the same wavelength from source node to the destination node, then the QoT of the lightpath is checked. It is performed in Algorithm 3 by the $QoT(t_x, t_y, \lambda_i, \pi)$ function, which returns 1 if the optical signal-to-noise-ratio (OSNR) (in both directions) of the lightpath linking the nodes t_x and t_y in wavelength λ_i is above a minimum threshold, or returns 0, otherwise. In the first case, the lightpath is established in all-optical manner in the route π using the wavelength found by the WA algorithm. If the QoT is not acceptable, the RA algorithm is executed, triggered by unacceptable signal quality. We name this RA as *RA_tQoT* which is executed to determine in which nodes that belong to the route π the signal must be regenerated.

If the WA algorithm fails to find a single available wavelength from source node to the destination node in route π, it means that wavelength conversion is needed in order to establish the call. Then, a regeneration triggered by the wavelength contention is executed. We name this function as *RA_tWC*. It tries to use the installed electronic infrastructure to perform the wavelength conversion. Note that both $RA\_tQoT(x,y,\lambda_i,\pi)$ and $RA\_tWC(x,y,\pi)$ are recursive functions applied to the route π. A call for either $RA\_tQoT(x,y,\lambda_i,\pi)$ or $RA\_tWC(x,y,\pi)$ with $x = 1$ (source node) and $y = 2$ (closest node to the source) is used for start the recursive procedure.

Algorithm 3 Translucent CAC

1: Arrival of a call request.
2: Execute the Routing algorithm which results in a route π ($\pi = \{t_1, t_2, ..., t_Z\}$) composed by Z nodes linking the source node (t_1) to the destination node (t_Z).
3: Execute the wavelength assignment algorithm in the selected route π.
4: **if** (There is a single wavelength available λ_i from the source node to the destination node in the route π) **then**
5: **if** ($QoT(t_1, t_Z, \lambda_i, \pi) = 1$) **then** {Regeneration is not required}
6: Establish the incoming call in route π and wavelength λ_i. {All-optical lightpath is established}
7: **else** {Regeneration is required}
8: *RA_tQoT*(1,2,λ_i,π) {Regeneration triggered by unacceptable signal quality}
9: **end if**
10: **else** {Regeneration is required}
11: *RA_tWC*(1,2,π) {Regeneration triggered by the wavelength contention}
12: **end if**

Algorithm 4 *RA_tQoT*(x,y,λ_i,π)

1: **if** $y = Z$ **then**
2: End algorithm.
3: **end if**
4: **if** ($f_y = 0$) **then** {no regenerator is available at node t_y}
5: *RA_tQoT*(x,$y+1$,λ_i,π). {Try to reach the next node}
6: **end if**
7: **if** ($QoT(t_x, t_y, \lambda_i, \pi) = 1$), **then** {QoT is acceptable}
8: *RA_tQoT*(x,$y+1$,λ_i,π). {Try to reach the next node}
9: **else** {Regeneration is required}
10: **if** ($\exists k$ such that $f_k \neq 0$ and $x < k < y$) **then**
11: *Regenerate* the signal at the node t_k closest to t_y along the π route such that $f_k \neq 0$.
12: *RA_tQoT*(k,$k+1$,λ_i,π).
13: **else**
14: The signal cannot be regenerated (i.e. the call request is blocked).
15: Stop.
16: **end if**
17: **end if**

Algorithm 5 *RA_tWC*(x,y,π)

1: **if** $y = Z$ **then**
2: End algorithm.
3: **end if**
4: **if** $f_y = 0$ **then** {no regenerator is available at node t_y}
5: *RA_tWC*(x,$y+1$,π). {Try to reach the next node}
6: **end if**
7: **if** ($\exists\lambda$ such that $QoTW(t_x, t_y, \lambda, \pi) = 1$), **then**
8: RA(x,$y+1$). {Try to reach the next node}
9: **else** {Regeneration is required}
10: **if** ($\exists k$ such that $f_k \neq 0$ and $x < k < y$) **then**
11: *Regenerate* the signal at the node t_k closest to t_y such that $f_k \neq 0$.
12: *Assign* the wavelength λ such that $QoTW(t_x, t_k, \lambda) = 1$ using FF
13: *RA_tWC*(k,$k+1$,π)
14: **else**
15: The signal cannot be regenerated (i.e., the call request is blocked).
16: Stop.
17: **end if**
18: **end if**

The *RA_tQoT*(x,y,λ_i,π) has four input parameters: a given route π, the indexes x and y (indexes of the route π) of two nodes that belong to π and the wavelength λ_i found by the WA algorithm. The pseudocode for this algorithm is depicted in the Algorithm 4. In this pseudocode, f_i stands for the available number of regenerators at node i. When the *RA_tQoT*(x,y,λ_i,π) is invoked, it mean that there is a route and a wavelength available from source to the destination node, nevertheless with a OSNR below the minimum threshold. Thus, this procedure tries to establish the entire lightpath in the wavelength λ_i found by the WA algorithm (no wavelength conversion is performed). Furthermore, it tries to use regenerators at the farthest possible node from the source node, splitting the lightpath in multiple all-optical segments linked by electronic regenerators in the segment edges. The QoT for each all-optical segment is checked before the establishment of the lightpath (see Sect. 5.2).

On the other hand, if *RA_tWC*(x,y,π) is invoked, there is no single wavelength available from source node to the destination node in the same frequency. The *RA_tWC*(x,y,π) has three input parameters: the indexes x and y of two nodes in the route π (which determines the sub-route currently under analysis) and the route π. Since a different wavelength can be assigned for each transparent segment, no wavelength is given as an input parameter. The pseudocode for function *RA_tWC*(x,y,π) is provided in the Algorithm 5. This algorithm tries to use regenerators at the farthest possible node from the source node, splitting the lightpath in multiple all-optical segments linked by electronic regenerators in the segment edges. In addition, a wavelength conversion is performed from one transparent segment to the next one. Again, the QoT for each all-optical segment is checked before the establishment of the lightpath. In this algorithm, the $QoTW(t_x, t_y, \lambda, \pi)$ function returns 1, if there is an available wavelength λ between the nodes t_x and t_y along the route π in both directions, that satisfies the QoT requirement, or returns 0, otherwise.

5 Simulation framework

We used a simulation framework in order to study the effectiveness of the proposed RP algorithms in the network operation phase. Some parts of the simulation framework described here are also used in the network planning stage of the RP algorithms. In this section, we discuss the important topics related to the simulation environment.

5.1 Physical layer impairments (PLI) modeling

In this subsection, we briefly describe the formulation used to evaluate the signal transmission quality impaired by physical effects. We used a version of the SIMTON simulator [26] for translucent networks to assess the network performance. The SIMTON simulator uses the physical layer model proposed by Pereira et al. [27] that quantifies the OSNR degradation and the pulse broadening along the optical signal propagation in an all-optical lightpath. The following impairments are considered in this paper: the spontaneous source emission (SSE) noise at optical transmitter, the ASE noise and the amplifier gain saturation effect, the homodyne crosstalk in optical switches, the PMD, the residual dispersion (RD), the four wave mixing (FWM) generated in the optical fibers, and the losses of the optical devices. The RD effect was taken into account as described in [26,28]. In this paper, we consider a link composed by a single span, which has the following elements: transmitter, optical switch, multiplexer, booster amplifier, optical fiber, pre-amplifier, demultiplexer, optical switch, and receiver. We assumed that dispersion compensation modules are installed at the amplification sites. The node architecture is shown in Fig. 1 and is similar to the one described in [6].

For each lightpath LP, the physical impairments model returns two values: $OSNR(LP)$, which stands for the OSNR at the destination node of the lightpath LP and $\Delta t(LP)$, which stands for the output pulse broadening of the optical signal in the lightpath LP.

5.2 Network simulation engine (NSE) and QoT thresholds

For each network simulation a set of calls is generated. The call arrivals follow a Poisson's process and the call hold time (i.e., the amount of time that the call is kept in the network) follows an exponential distribution. It characterizes a dynamic lightpath establishment (DLE). The multiplication of the average value of the call hold time by the average value of the rate of call arrivals results in the network load, given in erlang. The source-destination pairs of each call are chosen randomly by using an uniform probability density function. A candidate lightpath for the incoming call request is searched by the RWA module. In this paper, we use the shortest path as the routing algorithm and the first fit policy to assign the wavelengths.

Given a transparent segment, the QoT is checked in both direction since we consider a bidirectional lightpath establishment of the lightpaths. The QoT of a transparent segment is evaluated using the $OSNR(LP)$ and $\Delta t(LP)$ provided by the PLI modeling (Sect. 5.1). The current state of the network is considered in this evaluation. Our simulator checks if both QoT constraints are satisfied:

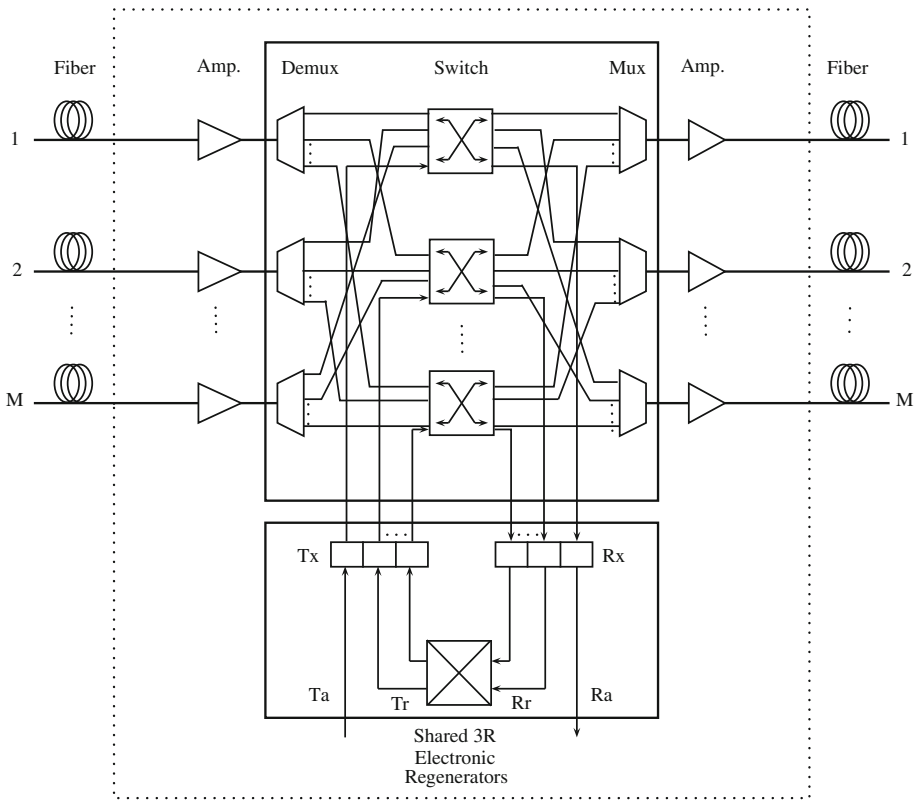

Fig. 1 Translucent wavelength routing node

Table 1 Default simulation parameters

Parameter	Value	Description
α	0.2 dB/km	Fiber loss coefficient
Δt_{QoT}	0.10	Maximum pulse broadening
$\Delta\lambda_{Tx}$	0.013 nm	Transmitter linewidth
λ_i	1, 528.77 nm	The first wavelength of the grid
λ_0	1, 450 nm	Zero dispersion wavelength for transmission fiber
λ_{0RD}	1, 528.77 nm	Zero residual dispersion wavelength
ε	−38 dB	Switch isolation factor
B_o	100 GHz	Optical filter bandwidth
B	40 Gbps	Transmission bit rate
D_{DCF} (@1,550 nm)	−110 ps/km nm	Compensating fiber dispersion coefficient
D_{PMD}	0.04 ps/$\sqrt{\text{km}}$	PMD coefficient
D_{Tx} (@1,550 nm)	4.5 ps/km nm	Transmission fiber dispersion coefficient
F_o (NF)	3.548 (5.5 dB)	Amplifier noise factor for low input optical powers (noise figure)
L_{Mx}	2 dB	Multiplexer loss
L_{Dx}	2 dB	Demultiplexer loss
L_{Sw}	2 dB	Optical switch loss
P_{Sat}	20 dBm	Amplifier output saturation power
P_{in}	3 dBm	Transmitter optical power
S_{DCF} (@1,550 nm)	−1.87 ps/km nm^2	Compensating fiber dispersion slope
S_{Tx} (@1,550 nm)	0.045 ps/km nm^2	Transmission fiber dispersion slope
W	24/36	Number of wavelengths in an optical link for Pacific Bell/ USA topology
$OSNR_{in}$	40 dB	Input optical signal-to-noise ratio
$OSNR_{QoT}$	20 dB	Optical signal-to-noise ratio for QoT criterion

$$OSNR(LP) > OSNR_{QoT} \tag{2}$$

and

$$\Delta t(LP) < \Delta t_{QoT}, \tag{3}$$

where $OSNR_{QoT}$ is the minimum acceptable OSNR value and Δt_{QoT} is the maximum pulse broadening for the QoT criterion. If either inequality does not hold, then the call request is blocked. An accepted call results in the establishment of a circuit switched bidirectional connection in two different fibers between the selected source and destination nodes. The blocking probability is obtained by the ratio of the number of blocked calls and the number of call requests. The Table 1 shows the default simulation parameters used for the simulations.

6 Simulation results

The MU-RP and MSU-RP algorithms obtain a solution for the number of regenerators that is placed in each network node. By using this solution (i.e., a translucent network), we perform simulations to obtain the network blocking probability. Therefore, the RP algorithms performance metrics are network blocking probability and the number of regenerators in the network. We compare our proposals MU-RP and MSU-RP with two others RP algorithms reported in the literature: NDF and SQP [6]. Our proposed RA algorithm is used to evaluate the blocking probability of all RP algorithms. The topologies used for the simulation are: the Modified Pacific Bell, depicted in Fig. 2 and composed by 17 nodes and 23 links, and the American Topology, depicted in Fig. 3 and composed by 61 nodes and 76 links. They are similar to the ones described in [6].

Figure 4 shows the results obtained for the modified Pacific Bell topology showing the blocking probability as a function of the total number of regenerators. The following four RP algorithms are compared: NDF (squares) and SQP (circles) proposed in [6], and our proposals MU-RP (up triangles) and MSU-RP (down triangles). The results were obtained for three different numbers of translucent nodes ($N = 3$, 6 and 9), which is equal for all RP algorithms, except for MSU-RP. The number of translucent nodes for MSU-RP is not an input variable, it is determined by

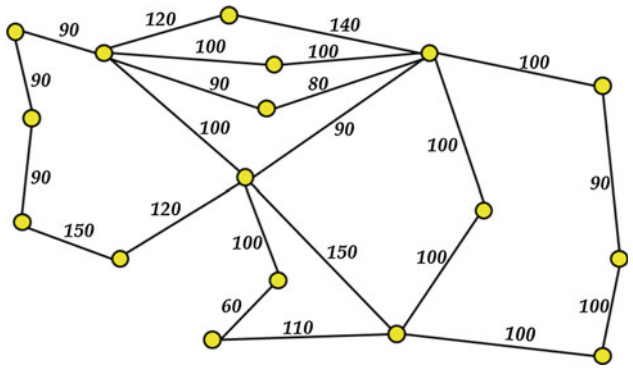

Fig. 2 Network topology 1. Link length in kilometers

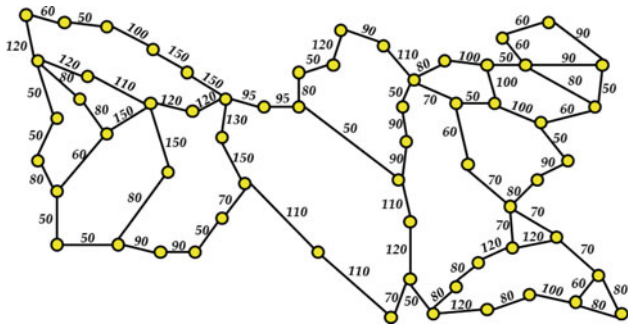

Fig. 3 Network topology 2. Link length in kilometers

algorithm itself. The number of translucent nodes found by MSU-RP for each simulation point is presented by a number inside the square close to the respective symbol. The simulation points of MSU-RP, which is not depicted in Fig. 4 with a square indicating the number of translucent nodes found for this respective point have the same number of translucent nodes found by the closest left neighbor simulation point. The comparison between MSU-RP and the other algorithms is fair since the results are plotted for the same total number of regenerator deployed. This can be achieved by setting $R = N \cdot X$, as discussed previously. In addition, we performed simulations for three network load values, 50, 60 and 80 erlangs. The blocking probability levels for the transparent and for the opaque operation of the network are also indicated in the figure.

Figure 4 shows that the NDF algorithm has the worst performance. This can be explained by the fact that this algorithm is only based on physical topology, which means that no traffic information is used during the RP decision. The three other algorithms are traffic-based RP strategies. For $N = 3$ (Fig. 4a, b, c), SQP outperforms MU-RP for any number of regenerators in the network and outperforms MSU-RP when the number of regenerators is less than 36 for a load of 50 erlangs and less than 48 regenerators for loads of 60 and 80 erlangs. For $N = 6$ (Fig. 4d, e, f) and $N = 9$ (Fig. 4g, h, i), MU-RP outperforms SQP, whereas MSU-RP outperforms all other algorithms. We observe a saturation value in the total number of regenerators in the network for all algorithms. This means that it is not worth to use more regenerator than the number indicated by these values, because the network performance is not improved significantly. One should observe that the MSU-RP algorithm achieves the opaque blocking probability level for almost all cases (excepted for $N = 3$ and $N = 6$ with Load $= 80$). The MU-RP and SQP algorithm only achieves the opaque level of blocking probability for $N = 9$. The NDF is not able to achieve the opaque level in terms of blocking probability for any of the investigated cases.

In Fig. 4e, we can observe that MSU-RP algorithm reaches the opaque network blocking level with only 118 regenerators, while the opaque configuration requires 1,104 electronic devices. This number is obtained by multiplying the number of wavelengths in each link by the sum of the degrees of the nodes [6]. This means that the translucent network configuration found by MSU-RP uses only 11 % of the number of regenerators required by the opaque network to achieve the same blocking probability level.

The result of a RP algorithm is the number of regenerators to be placed in each node of the network. We selected some obtained solutions (circled points in Fig. 4e) to illustrate the network configuration. The regenerators distributions found by each RP algorithm for these considered points are depicted in Fig. 5a. In this figure, each node that was selected to have regeneration capability by the NDF, SQP and MU-RP algorithms are marked, respectively, with a square, a circle and a up triangle. The algorithms NDF, SQP and MU-RP placed 120 regenerators equally distributed in 6 translucent nodes over the network, which means 20 devices in each selected node. The number inside the nodes represents the number of regenerators placed in each node by the MSU-RP algorithm. The MSU-RP algorithm placed 118 regenerators in 10 different nodes.

The configuration shown in Fig. 5a was used to obtain the results presented in the Fig. 6a, which depicts the blocking probability for the network configuration defined by each RP algorithm as a function of the network load. Figure 6a shows that the relative performance between the investigated algorithms is not affected (the better algorithm remains better and the worst remains worst) as the network load is varied. However, the differences between algorithms tends to increase as the network load decreases.

The same methodology was applied to the American Topology. Figure 7 shows the results obtained for the blocking probability as a function of the number of regenerators placed in the network. The blocking probability level of the transparent and opaque networks are also shown. The results were obtained for three different numbers of translucent nodes ($N = 20$, 30 and 40), which is equal for all RP algorithms, except for MSU-RP. The number of translucent

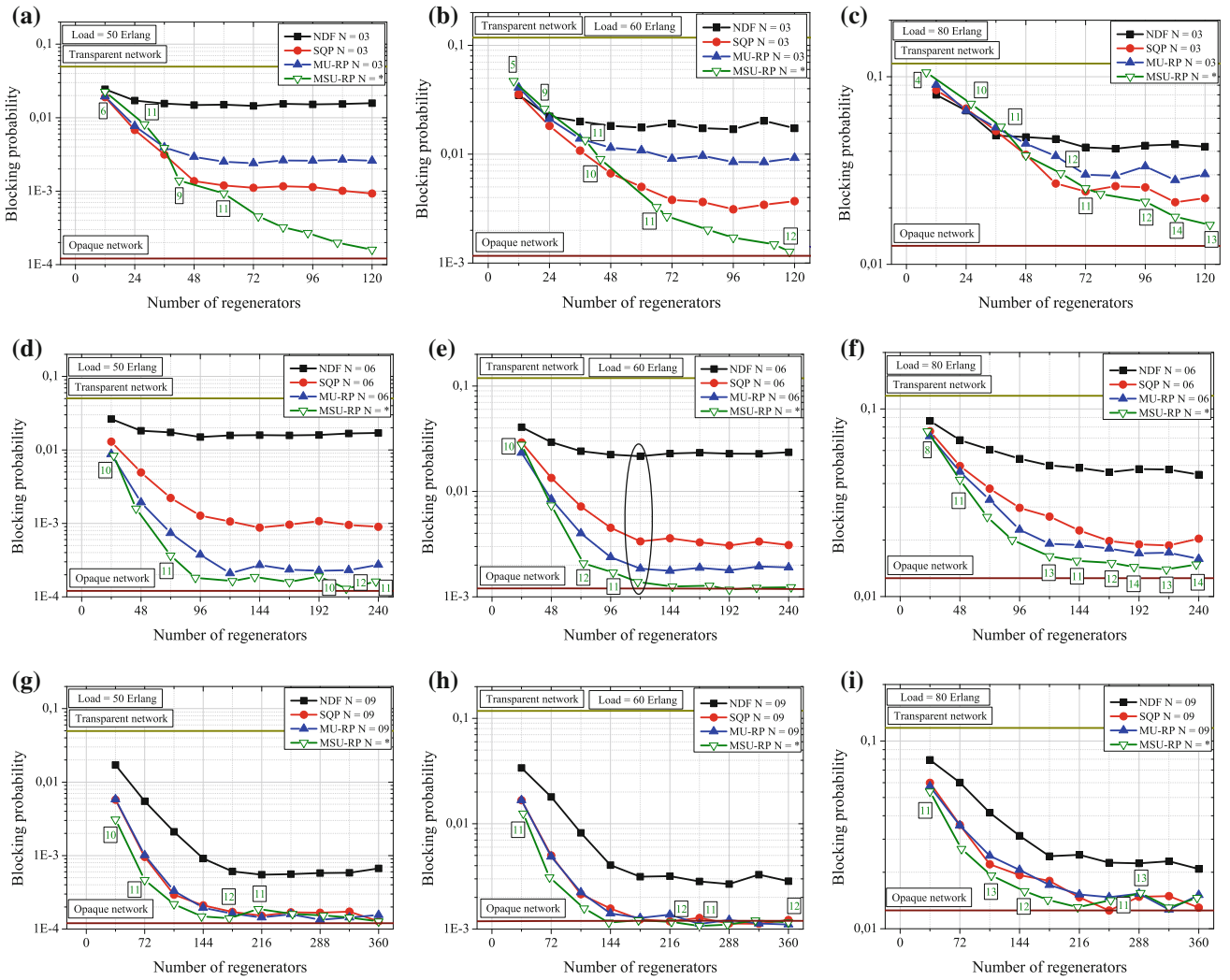

Fig. 4 Blocking probability as a function of the number of regenerators for the different RP algorithms, for topology 1, considering different loads and numbers of translucent nodes: **a** Load = 50 erlangs and $N = 3$, **b** Load = 50 erlangs and $N = 6$, **c** Load = 50 erlangs and $N = 9$, **d** Load = 60 erlangs and N = 3, **e** Load = 60 erlangs and $N = 6$, **f** Load = 60 erlangs and $N = 9$, **g** Load = 80 erlangs and $N = 3$, **h** Load = 80 erlangs and $N = 6$, **i** Load = 80 erlangs and $N = 9$. In the case of the MSU-RP, this value is shown inside the *squares* for each solution

nodes found by the MSU-RP algorithm is depicted in the same way as it is depicted in Fig. 4. Three load values were simulated, namely 60, 80 and 100 erlangs.

Figure 7 shows that again the NDF algorithm has the worst performance in comparison with all others RP algorithms for all investigated cases. The MU-RP algorithm outperforms SQP algorithm for almost all investigated cases. Again, one can observe a saturation value for the blocking probability when the total number of regenerators increases above a certain amount. One can also observe that the MSU-RP algorithm far outperformed the other algorithms and it achieved the opaque blocking probability level for all investigated cases. In addition, MSU-RP is the only algorithm that was able to reach the opaque blocking probability level.

In Fig. 7d, we observe that MSU-RP algorithm reaches the opaque network blocking level with 718 regenerators. The opaque configuration for this network requires 5,472 regenerators. This means that the translucent network configuration found by MSU-RP uses only 13 % of the number of regenerators needed by the opaque network.

Figure 5b shows the regenerators distributions found by each RP algorithm for the circled points in Fig. 7d. The algorithms NDF, SQP and MU-RP placed 720 regenerators equally distributed, 24 devices in 30 nodes over the network, whereas MSU-RP deployed 718 regenerators in 58 nodes.

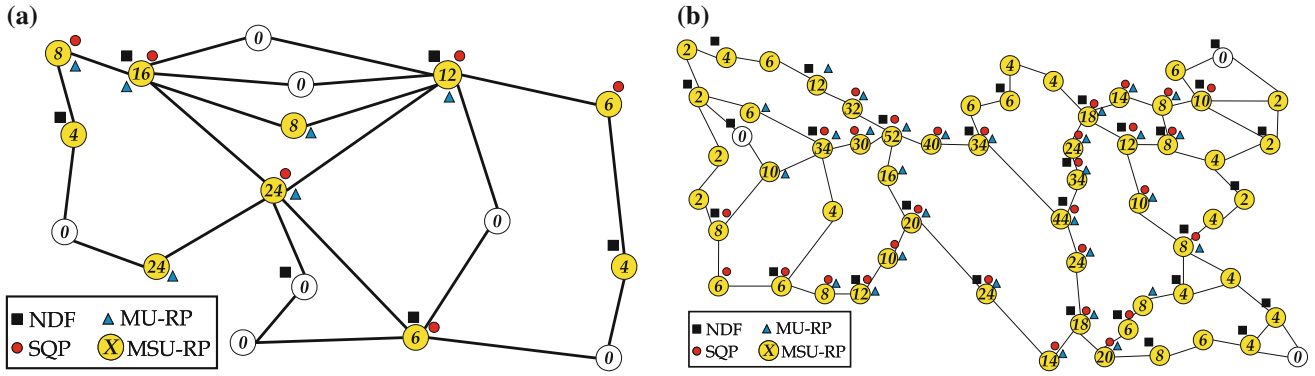

Fig. 5 The selected nodes by each RP algorithms for: **a** the modified Pacific Bell topology for the points highlighted (*circled*) in Fig. 4e and **b** the American Topology for the points highlighted (*circled*) in Fig. 7e. *Squares, circles* and *up triangles* indicate the nodes selected, respectively, by the NDF, SQP and MU-RP algorithms. For these, last three $N = 20$ regenerators are placed in each selected node. *Numbers* inside the nodes indicate the number of regenerators placed in each node by the MSU-RP algorithm

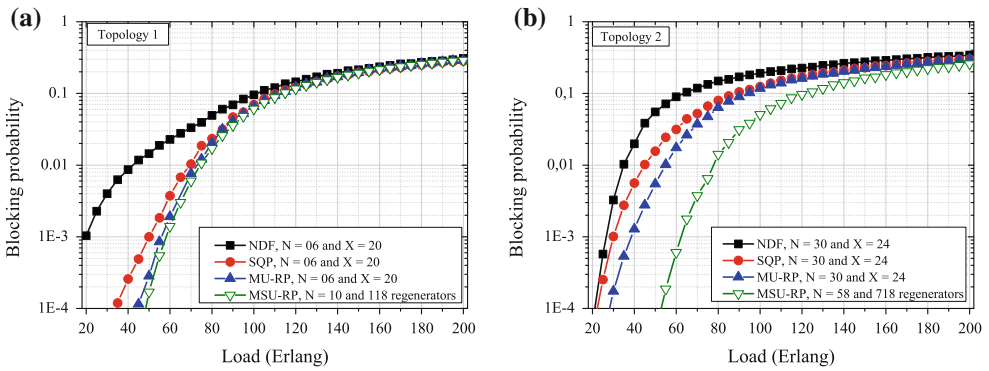

Fig. 6 Results for the network blocking probability as a function of the total network load (uniform traffic) considering the translucent networks designed by each RP algorithm for: **a** The Pacific Bell Topology (circulated solutions in Fig. 4e). **b** The American Topology (circulated solutions in Fig. 7d)

The configurations shown in Fig. 5b were used to obtain the results presented in the Fig. 6b, which depicts the blocking probability for the network configuration defined by each RP algorithm as a function of the network load. Figure 6b shows that the relative performance between the investigated algorithms is not affected again.

6.1 Performance analysis under a non-uniform traffic pattern

The RP solution found by our proposals MU-RP and MSU-RP are obtained for a given traffic load distribution. The results shown in Fig. 6 indicate that the MU-RP and MSU-RP algorithms present better performance than the others in the uniform traffic distribution scenario, even when we vary the network load. It indicates that both algorithms are robust to deal with variations in the total network load that may occur along the time. Nevertheless, it is also worthy to investigate the robustness of the MU-RP and MSU-RP algorithms when the online traffic load distribution varies after the regenerator placement. In order to verify it, we investigated the algorithms performance as a function of the variation in the load distribution among nodes of the network.

Given a uniform traffic matrix $T = \{\rho_{ij}\}$, we produce a variation in this traffic matrix (i.e., $T' = \{\rho'_{ij}\}$), which simulates the traffic distribution fluctuation along the day. T' is evaluated from T by the multiplication of each entry by a random number: $\rho'_{ij} = (1+r)\cdot\rho_{ij}$, where r is a random number with a uniform distribution in the $[-R, R]$ interval and R is the maximum allowed load variation per source-destination pair. The T' matrix is normalized to keep the same total network load of the matrix T. Hence, $R = 0$ corresponds to the case of uniform traffic, whereas $R \neq 0$ corresponds to a non-uniform traffic. $R = 0.5$ represents the case of the traffic load of a given source-destination pair may increase or decrease by at most 50 % of its traffic in the uniform case.

We performed a statistical analysis of the behavior of the blocking probability of the MU-RP and MSU-RP algorithms when compared to the other algorithms. For this purpose, we generated a set of 30 different and independent traffic

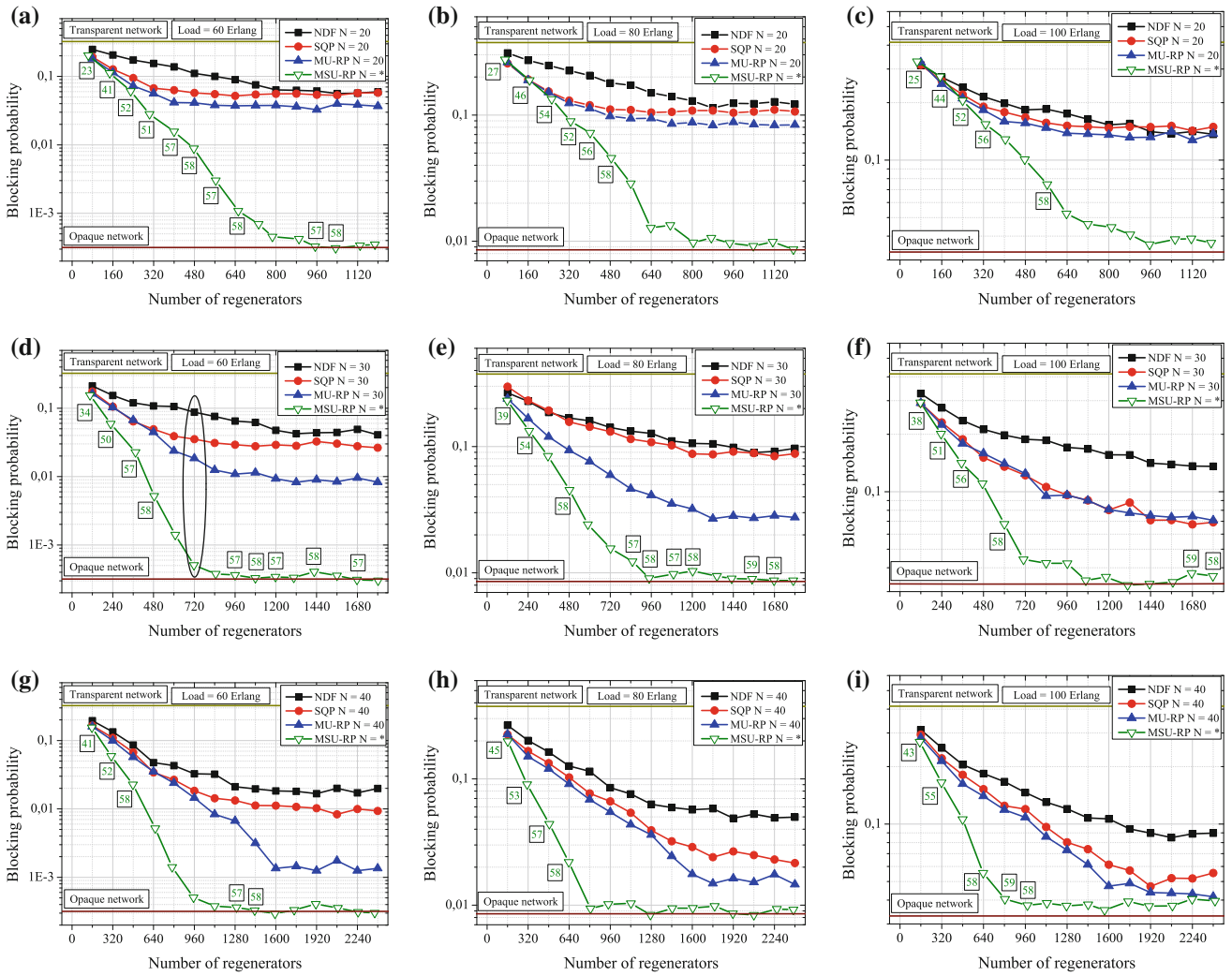

Fig. 7 Blocking probability as a function of the number of regenerators for the different RP algorithms, for topology 1, considering different loads and numbers of translucent nodes: **a** Load = 50 erlangs and $N = 3$, **b** Load = 50 erlangs and $N = 6$, **c** Load = 50 erlangs and $N = 9$, **d** Load = 60 erlangs and $N = 3$, **e** Load = 60 erlangs and $N = 6$, **f** Load = 60 erlangs and $N = 9$, **g** Load = 80 erlangs and $N = 3$, **h** Load = 80 erlangs and $N = 6$, **i** Load = 80 erlangs and $N = 9$. In the case of the MSU-RP, this value is shown inside the *squares* for each solution

matrixes. For each of these matrixes, we obtained the blocking probability from each considered RP algorithms. The Fig. 8 shows the blocking probability for each considered RP algorithms in terms of a box and whiskers chart for three different values of R, $R = 0.2$, $R = 0.5$ and $R = 1$. The box stands for the 50 % of the obtained data, the whiskers correspond to the 100 % of the obtained data. The open symbols stand for the mean value and the horizontal line inside the box is the median. The closed symbols at the left side of the box is the blocking probability of a given algorithm obtained for the uniform traffic case. The total network load is kept constant at a value of 60 erlangs, independently of the considered value for R. The 30 different matrixes are simulated in the same regeneration scenario found in Fig. 5.

One can note that the deviation observed for non-uniform traffic (box chart), when compared to the result obtained for uniform traffic (closed symbols), have almost the same magnitude for all investigated algorithm. Note that as we are randomly changing the traffic matrix, in some cases, the new matrix may increase the load in less congested routes and decrease the load in more congested routes, leading to a lower network blocking probability. In some other cases, the new generated matrix may do the opposite, leading to a higher network blocking probability. This explains the variation of blocking probability observed for all algorithms in Fig. 8, especially for high values of R. Clearly, the average performance of the RP algorithms, given by the symbols in Fig. 8, did not change significantly from the uniform traffic case

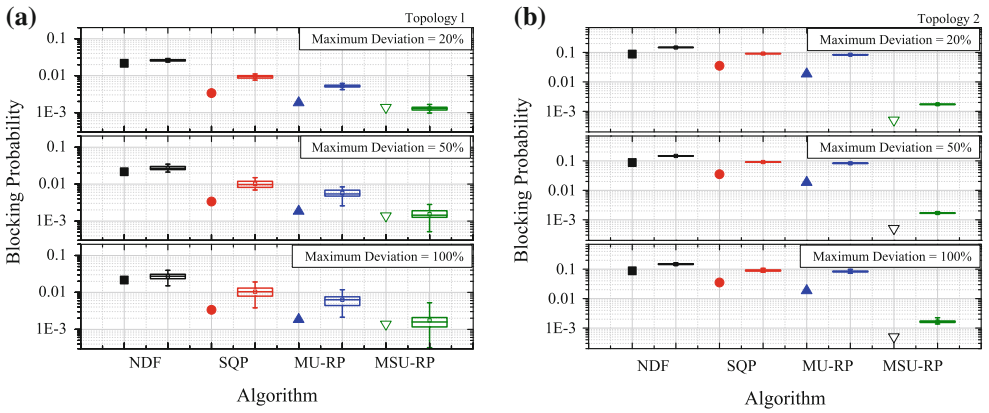

Fig. 8 Blocking probability as a function of RP algorithms, considering non-uniform traffic with different values of maximum load deviation (*box plots*) and uniform traffic (*symbols*) for the: **a** Pacific Bell Topology and **b** American Topology

($R = 0$) to the non-uniform traffic cases. These results show no indication that our proposed RP algorithms could perform poorly if the traffic distribution in the network is different from the one used in the offline simulations for regenerator placement. The results shown in Fig. 8 indicate that the proposed RP algorithms are also robust enough to deal with load distribution variations that may occur in the network during the course of the day.

7 Conclusion

In this paper, we proposed an extension for existing heuristic algorithms for the regenerator assignment problem and two heuristic algorithms to tackle the regenerator placement problem based on the network traffic. The MSU-RP algorithm outperformed all other algorithms, whereas MU-RP outperformed NDF in all cases and outperformed SQP in most of the investigated cases. MSU-RP reached the opaque blocking probability level using only 11 %, for the modified Pacific Bell Topology, and 13 %, for the American Topology, of the total number of regenerators needed for the opaque network. We also observed that for a larger network (i.e., American Topology), only the MSU-RP algorithm was able to reach the opaque blocking probability level.

Our results show that from the performance point of view (blocking probability) and CAPEX point of view (total number of regenerators), it is better to distribute fewer regenerators in more nodes, as MSU-RP does, than use a fixed number of regenerators (pool) to distribute in fewer translucent nodes, as the other RP algorithms do. However, the network solution found by the MSU-RP algorithm shows a higher operational cost (OPEX) since it requires a larger number of translucent nodes. Therefore, depending on the target network, it may be a better solution to increase the network OPEX in order to improve the network performance (i.e., profit vs cost analysis).

In addition, we also investigated the performance of all considered algorithms for uniform and non-uniform traffics. We found that the relative performance of the algorithms is almost unaltered when different load patterns are considered.

Acknowledgments The authors acknowledge the financial support from FACEPE, CNPq, CAPES, UPE, and UFPE for scholarships and grants.

References

[1] Desurvire, E.B.: Capacity demand and technology challenges for lightwave systems in the next two decades. J. Lightw. Technol. **24**(12), 4697–4710 (2006)
[2] Ramaswami, R., Sivarajan, K.N., Sasaki, G.: Optical Networks: A Practical Perspective, 3rd edn. Morgan Kaufmann, Waltham (2010)
[3] Shen, G., Tucker, R.S.: Translucent optical networks: the way forward. IEEE Commun. Mag. **45**(2), 48–54 (2007)
[4] Karasan, E., Arisoylu, M.: Design of translucent optical networks: partitioning and restoration. Photon. Netw. Commun. **8**(2), 209–221 (2004)
[5] Shen, G., Sorin, W.V., Tucker, R.S.: Cross-layer design of ASE-noise-limited island-based translucent optical networks. J. Lightw. Technol. **27**(11), 1434–1442 (2009)
[6] Yang, X., Ramamurthy, B.: Sparse regeneration in translucent wavelength-routed optical networks: Architecture, network design and wavelength routing. Photon. Netw. Commun. **10**(1), 39–53 (2005)
[7] Ye, Y., Chai, T., Cheng, T., Lu, C.: Algorithms for the design of WDM translucent optical networks. Opt. Exp. **11**(22), 2917–2926 (2003)
[8] Flammini, M., Marchetti-Spaccamela, A., Monaco, G., Moscardelli, L., Zaks, S.: On the complexity of the regenerator placement problem in optical networks. IEEE/ACM Trans. Netw. **19**(2), 498–511 (2011)
[9] Sambo, N., Andriolli, N., Giorgetti, A., Castoldi, P., Bottari, G.: Multiple path based regenerator placement algorithm in translucent optical networks. In: 11th International Conference on Transparent Optical Networks (ICTON), July 2009, pp. 1–4

[10] Manousakis, K., Kokkinos, P., Christodoulopoulos, K., Varvarigos, E.: Joint online routing, wavelength assignment and regenerator allocation in translucent optical networks. J. Lightw. Technol. **28**(8), 1152–1163 (2010)
[11] Ye, Y., Chai, T.Y., Cheng, T.H., Lu, C.: Dynamic routing and wavelength assignment algorithms in wavelength division multiplexed translucent optical networks. Comput. Commun. **29**(15), 2975–2984 (2006)
[12] Ye, Y., Cheng, T., Lu, C.: Novel algorithm for upgrading of translucent optical networks. Opt. Exp. **11**(23), 3022–3033 (2003)
[13] Peng, Y., Hu, W., Sun, W., Wang, X., Jin, Y.: Impairment constraint multicasting in translucent WDM networks: architecture, network design and multicasting routing. Photon. Netw. Commun. **13**(1), 93–102 (2007)
[14] Yang, X., Ramamurthy, B.: Sparse regeneration in a translucent WDM optical network. In: Proceedings of the SPIE - The International Society for Optical Engineering, January 2001, pp. 61–70
[15] Sambo, N., Andriolli, N., Giorgetti, A., Valcarenghi, L., Cugini, F., Castoldi, P.: Accounting for shared regenerators in GMPLS-controlled translucent optical networks. J. Lightw. Technol. **27**(19), 4338–4347 (2009)
[16] Chaves, D.A.R., Ayres, C.F.C.L.C., Carvalho, R.V.B., Pereira, H.A., Bastos-Filho, C.J.A., Martins-Filho, J.F.: Multiobjective sparse regeneration placement algorithm in optical networks considering network performance and capex. In: 12th International Conference on Transparent Optical Networks (ICTON), July 2010, pp. 1–4
[17] Chaves, D.A.R., Ayres, C.F.C.L.C., Carvalho, R.V.B., Pereira, H.A., Bastos-Filho, C.J.A., Martins-Filho, J.F.: Sparse regeneration placement for translucent optical networks using multiobjective evolutionary algorithms considering quality of service and capital cost. In SBMO/IEEE MTT-S International Microwave and Optoelectronics Conference (IMOC), November 2009, pp. 417–422
[18] Pachnicke, S., Paschenda, T., Krummrich, P.: Assessment of a constraint-based routing algorithm for translucent 10Gbits/s DWDM networks considering fiber nonlinearities. J. Optic. Netw. **7**(4), 365–377 (2008)
[19] Youssef, M., Al Zahr, S., Gagnaire, M.: Traffic-driven vs. topology-driven strategies for regeneration sites placement. In: IEEE International Conference on Communications (ICC), May 2010, pp. 1–6
[20] Youssef, M., Al Zahr, S., Gagnaire, M.: Cross optimization for RWA and regenerator placement in translucent WDM networks. In: 14th Conference on Optical Network Design and Modeling (ONDM), February 2010, pp. 1–6
[21] Chen, S., Ljubic, I., Raghavan, S.: The regenerator location problem. Networks **55**(3), 205–220 (2010)
[22] Kuipers, F., Beshir, A., Orda, A., Van Mieghem, P.: Impairment-aware path selection and regenerator placement in translucent optical networks. In: 18th IEEE International Conference on Network Protocols (ICNP), October 2010, pp. 11–20
[23] Rumley, S., Gaumier, C., Szymanek, R.: Multi-objective optimization of regenerator placement using constraint programming. In: 15th International Conference on Optical Network Design and Modeling (ONDM), February 2011, pp. 1–6
[24] Youssef, M., Al Zahr, S., Gagnaire, M.: Translucent network design from a capex/opex perspective. Photon. Netw. Commun. **22**, 85–97 (2011)
[25] Kim, S.W., Seo, S.W.: Regenerator placement algorithms for connection establishment in all-optical networks. IEE Proc. Commun. **148**(1), 25–30 (2001)
[26] Chaves, D.A.R., Bastos-Filho, C.A., Pereira, H.A., Martins-Filho, J.F.: SIMTON: a simulator for transparent optical networks. J. Commun. Inf. Syst. (JCIS), **25**(1), pp. 1–10 (2010). [Online]. Available: http://iecom.dee.ufcg.edu.br/~jcis/Abril%202010/index.html
[27] Pereira, H.A., Chaves, D.A.R., Bastos-Filho, C.J.A., Martins-Filho, J.F.: OSNR model to consider physical layer impairments in transparent optical networks. Photon. Netw. Commun. **18**(2), 137–149 (2009)
[28] Bastos-Filho, C.J.A., Chaves, D.A.R., e Silva, F.S.F., Pereira, H.A., Martins-Filho, J.F.: Wavelength assignment for physical-layer-impaired optical networks using evolutionary computation. J. Optic. Commun. Netw. **3**(3), 178–188 (2011)

Author Biographies

Daniel A. R. Chaves was born in Recife, Brazil, in 1981. He received the B.Sc. degree in electronics engineering from Federal University of Pernambuco (UFPE) in 2006. He received the M.Sc. and Ph.D degrees in electrical engineering from Federal University of Pernambuco (UFPE), in 2008 and 2012, respectively. He is a Professor of Computer Engineering Group (E-Comp) in the Polytechnic School of University of Pernambuco (UPE). Dr. Chaves is currently working with Research Group on Networks and Communications (UPE) and with Laboratory of Optical Networks (UFPE). His interests are related to lightwave communication systems, including high capacity WDM transmission, optical networking, impairment aware routing and wavelength assignment algorithms, design of all-optical and translucent networks and applications of computational intelligence in optical network optimization. Citation: http://scholar.google.com/citations?user=fM6l2AMAAAAJ&hl=en.

Renan V. B. Carvalho was born in Recife, Brazil, in 1987. He received the B.Sc. degree in Electronics Engineering from University of Pernambuco (UPE) in 2010. He is currently working towards the M.Sc. degree in Electrical Engineering at the Federal University of Pernambuco (UFPE). His interests are related to WDM optical networks including design of translucent and all-optical networks, regenerator placement problem, regenerator allocation algorithms and applications of computational intelligence in optical networks optimization.

Helder A. Pereira was born in Paulista, Brazil, in 1980. He received the B.Sc. degree in electronics Engineering from University of Pernambuco (UPE), Recife, Brazil, in 2000, the M.Sc. degree at Telecommunication National Institute (Inatel), Santa Rita do Sapucaí, Brazil, in 2002 and the Ph.D. degree in Electrical Engineering at the Federal University of Pernambuco (UFPE), Recife, Brazil, in 2007. He is a professor at the Electrical Engineering Department of University of Pernambuco (DEE-UPE).

Carmelo J. A. Bastos-Filho was born in Recife, Brazil, in 1978. He received the B.Sc. degree in Electronics Engineering from Federal University of Pernambuco in 2000. He received the M.Sc. and Ph.D. degrees in Electrical Engineering from UFPE, in 2003 and 2005, respectively. In 2006, he received the best Brazilian Thesis award in Electrical Engineering. His interests are related to optical networks, swarm intelligence, evolutionary computation, multi-objective optimization and biomedical applications. He is currently an associate professor at Polytechnic School of the University of Pernambuco. He is the head of the research division of the Polytechnic School of Pernambuco. He also coordinates the Masters course on Systems Engineering. He is a Senior member of IEEE (Institute of Electrical and Electronics Engineers), member of SBMO (Brazilian Microwave and Optoelectronics Society), SBrT (Brazilian Telecommunication Society), as well as a research fellow of the National Research Council of Brazil (CNPq) http://scholar.google.com/citations?user=t3A96agAAAAJ.

Joaquim F. Martins-Filho was born in Recife, Brazil, in 1966. He received the B.Sc. degree in Electronics Engineering from the Federal University of Pernambuco (UFPE), Recife, in 1989, and the M.Sc. degree in Physics from the same institution in 1991, studying nonlinear optics in optical fibers. He received his Ph.D. degree in Electronics Engineering from the University of Glasgow, Scotland, in 1995, investigating ultrafast optical pulse generation from mode-locked semiconductor quantum well lasers. Since 1998 he is an associate professor in the Photonics Group, Department of Electronics and Systems of UFPE, in Recife. His current interests are in devices, subsystems, transmission systems and networking for optical communications and optical sensors. Prof. Joaquim Martins-Filho is a Senior Member of IEEE (Institute of Electrical and Electronics Engineers), Member of OSA (Optical Society of America), SBMO (Brazilian Microwave and Optoelectronics Society), SBrT (Brazilian Telecommunication Society) and SBF (Brazilian Physics Society), as well as a Research Fellow of the National Research Council of Brazil (CNPq). Citations: http://scholar.google.com/citations?user=BqzbDdsAAAAJ.